Subcarrier Multiplexing for High-Speed Optical Transmission

Rongqing Hui, *Senior Member, IEEE*, Benyuan Zhu, Renxiang Huang, Christopher T. Allen, *Senior Member, IEEE*, Kenneth R. Demarest, *Senior Member, IEEE*, and Douglas Richards

***Abstract*—The performance of high-speed digital fiber-optic transmission using subcarrier multiplexing (SCM) is investigated both analytically and numerically. In order to reduce the impact of fiber chromatic dispersion and increase bandwidth efficiency, optical single-sideband (OSSB) modulation was used. Because frequency spacing between adjacent subcarriers can be much narrower than in a conventional DWDM system, nonlinear crosstalk must be considered. Although chromatic dispersion is not a limiting factor in SCM systems because the data rate at each subcarrier is low, polarization mode dispersion (PMD) has a big impact on the system performance if radiofrequency (RF) phase detection is used in the receiver. In order to optimize the system performance, tradeoffs must be made between data rate per subcarrier, levels of modulation, channel spacing between subcarriers, optical power, and modulation indexes. A 10-Gb/s SCM test bed has been set up in which 4 $\times$ 2.5 Gb/s data streams are combined into one wavelength that occupies a 20-GHz optical bandwidth. OSSB modulation is used in the experiment. The measured results agree well with the analytical prediction.**

***Index Terms*—Optical fiber communication, optical fiber polarization, optical modulation, optical receiver, optical signal processing, subcarrier multiplexing.**

I. Introduction

In order to use the optical bandwidth provided by optical fibers more efficiently, new transmission technologies have been developed in recent years, such as time division multiplexing (TDM), wavelength division multiplexing (WDM), and their combinations. Apart from noise accumulation, high-speed TDM optical systems suffer from chromatic dispersion, nonlinear crosstalk, and polarization-mode dispersion (PMD). Optical systems with data rates of 10 Gb/s and higher require precise dispersion compensation and careful link engineering. On the other hand, WDM technology spreads transmission capacity into various wavelength channels and uses relatively low data rates at each wavelength. However, due to the selectivity of optical filters and limitations in the wavelength stability of semiconductor lasers, the minimum channel spacing is $\sim$50 GHz in current commercial WDM systems. Narrower channel spacing has been pursued by industry and the research community to increase fiber transmission capacity. More sophisticated modulation formats may help to increase the bandwidth efficiency compared to the basic ON–OFF keying modulation.

Optical subcarrier multiplexing (SCM) is a scheme where multiple signals are multiplexed in the radiofrequency (RF) domain and transmitted by a single wavelength. A significant advantage of SCM is that microwave devices are more mature than optical devices; the stability of a microwave oscillator and the frequency selectivity of a microwave filter are much better than their optical counterparts. In addition, the low phase noise of RF oscillators makes coherent detection in the RF domain easier than optical coherent detection, and advanced modulation formats can be applied easily. A popular application of SCM technology in fiber optic systems is analog cable television (CATV) distribution [1], [2]. Because of the simple and low-cost implementation, SCM has also been proposed to transmit multichannel digital optical signals using direct detection [3], [4] for local area optical networks.

In this paper, we analyze the performance of high-speed digital fiber-optic transmission using SCM both analytically and numerically. In order to minimize the impact of fiber chromatic dispersion, optical single-sideband (OSSB) modulation is used, which also increases the optical bandwidth efficiency. Fiber nonlinearities such as cross-phase modulation (XPM) and four-wave mixing (FWM) may generate significant amounts of nonlinear crosstalk between adjacent SCM channels because they are very closely spaced. Although chromatic dispersion is not a limiting factor in OSSB-modulated SCM systems because the data rate at each subcarrier is relatively low, carrier fading due to PMD may be significant because of high subcarrier frequencies [14]. In order to optimize the system performance, tradeoffs must be made between data rate per subcarrier, levels of modulation, channel spacing between subcarriers, optical power, and modulation indexes. An experiment of 10-Gb/s SCM fiber-optical system was performed, in which 4 $\times$ 2.5 Gb/s data streams were combined into one wavelength, which occupied an approximately 20-GHz optical bandwidth. OSSB modulation was achieved using a balanced dual-electrode electrooptic modulator. This 10-Gb/s composite optical signal was transmitted over 150-km equivalent standard single-mode fiber (SMF) without any dispersion compensation [5]. The combination of SCM and WDM may provide a more flexible platform for high-speed optical transport networks with high optical bandwidth efficiency and high dispersion tolerance.

The basic configuration of an SCM–WDM optical system is shown in Fig. 1. In this example, n independent high-speed digital signals are mixed by N different microwave carrier

Manuscript received November 24, 2001; revised December 13, 2001. This work was supported in part by Sprint Communications Company, L.P.

R. Hui, B. Zhu, C. T. Allen, and K. R. Demarest are with the Information and Telecommunication Technology Center, Department of Electrical and Computer Science, University of Kansas, Lawrence, KS 66044 USA.

R. Huang was with the Information and Telecommunication Technology Center, Department of Electrical and Computer Science, University of Kansas, Lawrence, KS 66044 USA. He is now with Sprint Advanced Technology Laboratories, Burlingame, CA 94010 USA.

D. Richards is with Sprint, Inc., Overland Park, KS 66212 USA.

Publisher Item Identifier S 0733-8724(02)02190-4.

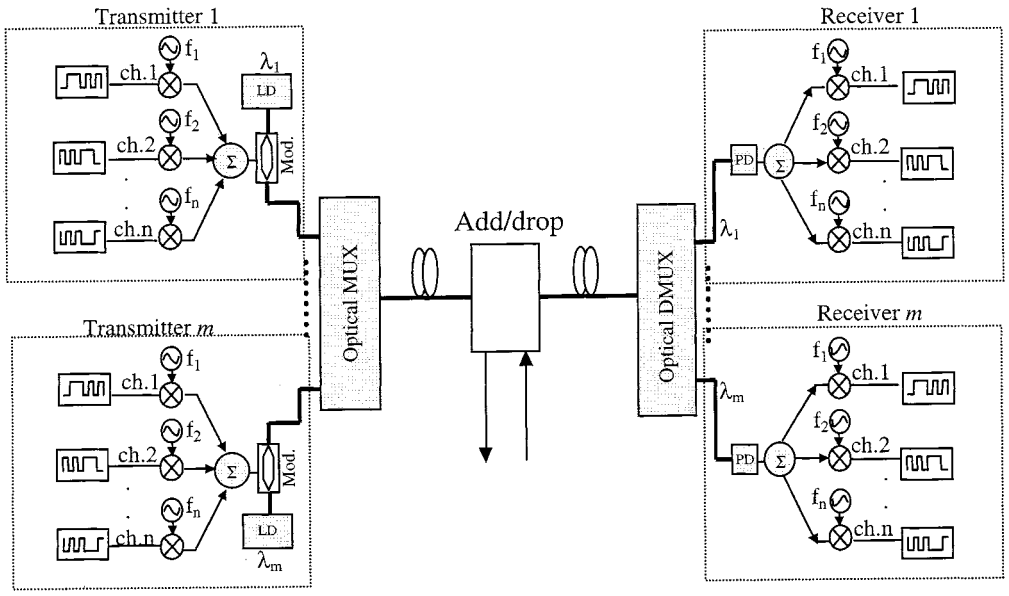

Fig. 1. SCM–WDM system architecture.

frequencies f_i. These are combined and optically modulated onto an optical carrier. m wavelengths are then multiplexed together in an optical WDM configuration. At the receiver, an optical demultiplexer separates the wavelengths for individual optical detectors. Then, RF coherent detection is used at the SCM level to separate the digital signal channels. Channel add–drop is also possible at both the wavelength and SCM levels. Although this SCM–WDM is, in fact, an ultradense WDM system, sophisticated microwave and RF technology enables the channel spacing to be comparable to the spectral width of the baseband, which is otherwise not feasible by using optical technology. Compared to conventional high-speed TDM systems, SCM is less sensitive to fiber dispersion because the dispersion penalty is determined by the width of the baseband of each individual signal channel. Compared to conventional WDM systems, on the other hand, it has better optical spectral efficiency because much narrower channel spacing is allowed.

Conventional SCM generally occupies a wide modulation bandwidth because of its double-sideband spectrum structure and, therefore, is susceptible to chromatic dispersion. In order to reduce dispersion penalty and increase optical bandwidth efficiency, optical SSB modulation is essential for long-haul SCM–WDM optical systems. Fortunately, optical SSB is relatively easy to accomplish in SCM systems. This is because there are no low-frequency components, and the Hilbert transformation is, thus, much simpler than OSSB in conventional TDM systems [6], [7].

II. Experiment

In order to investigate the feasibility of long-haul digital SCM transmission at high speed, an experiment was conducted at 10-Gb/s capacity per wavelength. Four 2.5-Gb/s digital signals were mixed with four RF carriers each at 3.6, 8.3, 13, and 18 GHz, and binary phase-shift keying (BPSK) modulation format was used in the RF domain. The RF carriers were then combined and amplified to drive a dual electrode $LiNbO_3$ Mach–Zehnder (MZ) modulator with a 20-GHz bandwidth. As shown in Fig. 2, in order to generate OSSB, the composite signal was applied to both of the two balanced electrodes with a $\pi/2$ phase shift in one of the arms using a 90° hybrid splitter. A direct current (dc) bias sets the modulator at the quadrature point to generate OSSB [8]. Fig. 3 shows the OSSB spectrum measured by a scanning Fabry–Perot (FP) interferometer with a 1-GHz

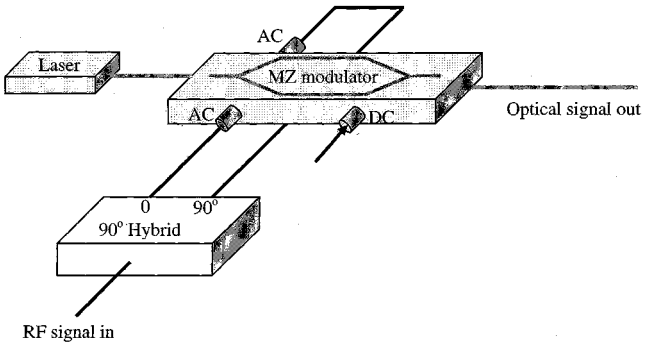

Fig. 2. Illustration of OSSB modulation using dual-electrode MZ modulator.

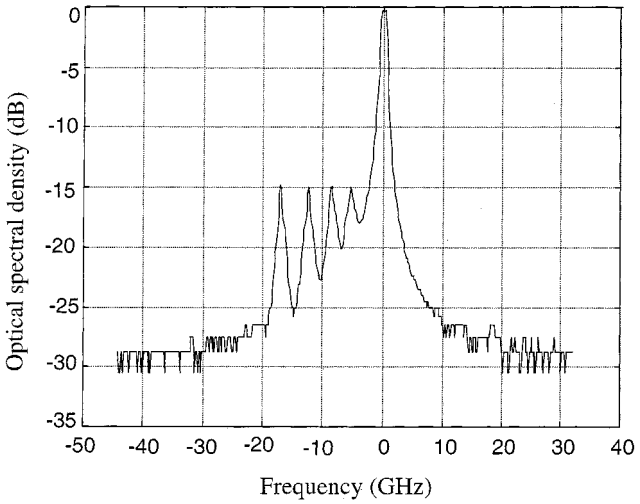

Fig. 3. Measured OSSB spectrum with four subcarrier channels.

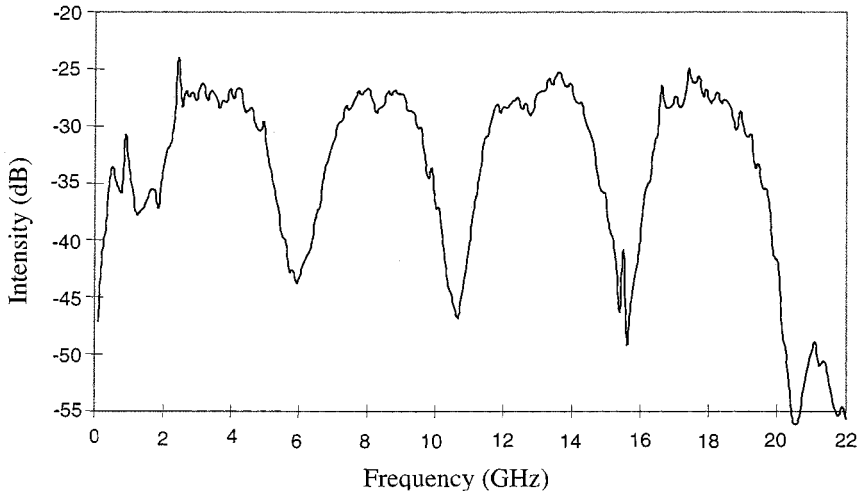

Fig. 4. Example of the measured RF composite spectrum at the receiver.

resolution bandwidth. Suppression of the unwanted sideband of at least 13 dB was achieved, as can be seen from Fig. 3.

To measure the transmission performance, this optical signal was then launched into an SMF link with accumulated chromatic dispersion of −2640 ps/nm, SMF. The experiment was performed using dispersion compensating fibers (DCF) (DK series, Lucent Technologies, Murray Hill, NJ 07974 USA), which have large negative dispersion values. No dispersion compensation was used. At the receiver, the optical signal was preamplified and detected by a wide-band photodetector. A typical spectrum of the detected composite RF signal after the wideband photodiode is shown in Fig. 4, where four optical subcarriers are converted into the RF domain. Each subcarrier was then down-converted to an individual baseband by mixing the composite signal with an appropriate RF local oscillator and then passing through a 1.75-GHz lowpass filter. Although both amplitude shift keying (ASK) and phase shift keying (PSK) modulation–detection schemes may be used; in our experiment, we have used PSK format in the RF domain for better receiver sensitivity.

The bit error rate (BER) was measured for all four channels, both back-to-back and over the fiber. Fig. 5 shows the measured BER plotted as a function of received optical power level. The measurement was performed under the condition that all four SCM channels were operated simultaneously. At the BER level of 10^{-10}, the back-to-back sensitivity ranges from −25 dBm to −27 dBm for the different channels due to the ripples in the microwave devices and the inaccuracy of the modulation index of each individual SCM channel. After transmission, the sensitivity is degraded by about 2.5 dB. In our experiment, this degradation was largely attributed to the frequency instability of the local oscillators. In this four-RF channel experiment, an approximately 4.7-GHz spacing between RF channels was used; this spacing was selected based on the tradeoff between the interchannel crosstalk and the bandwidth efficiency. In fact, the minimum allowed spacing between RF channels largely depends on the quality of the baseband filter. Fig. 6 shows the measured receiver sensitivity $(\text{BER} = 10^{-9})$ versus RF channel spacing. Significant sensitivity degradation results for channel

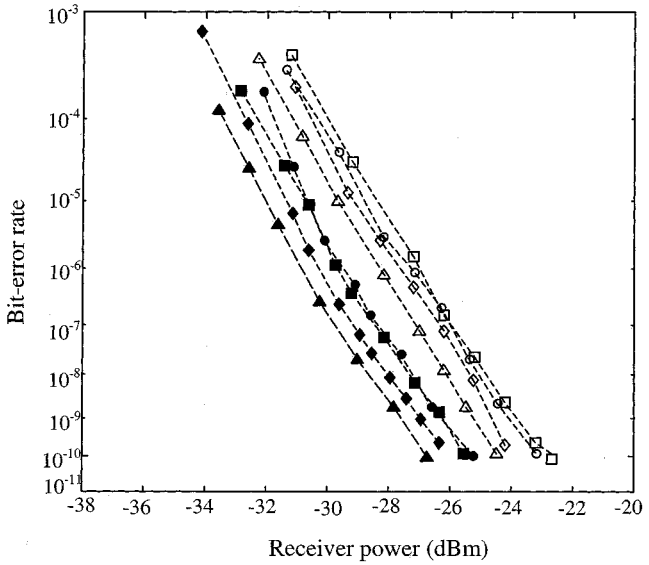

Fig. 5. Measured bit-error rate in a system with four subcarrier channels before (solid points) and after (open points) a fiber transmission line with a −2640 ps/nm total dispersion.

spacing of less than 4.7 GHz due to interchannel crosstalk. The results shown in Fig. 6 are for a case where only two subcarrier channels were used. Thus, the maximum allowable modulation index is higher than a four-channel case; therefore, the sensitivity in Fig. 6 is better than that in Fig. 5. Further improvement of bandwidth efficiency might be achieved using microwave single-sideband modulation.

Owing to the relatively low data rates carried by each individual SCM channel, the SCM system can tolerate more chromatic dispersion than a TDM system of same capacity. We have made an experimental comparison of the system performance between a TDM system with 192 optical combiners (OCs) and a four-channel OC-48 SCM system. Fig. 7 shows the measured receiver sensitivities versus the accumulated dispersion. Back to back, the sensitivity of SCM system is about 6-dB worse compared to its TDM counterpart because of small modulation index in the SCM system. However, with the accumulated dis-

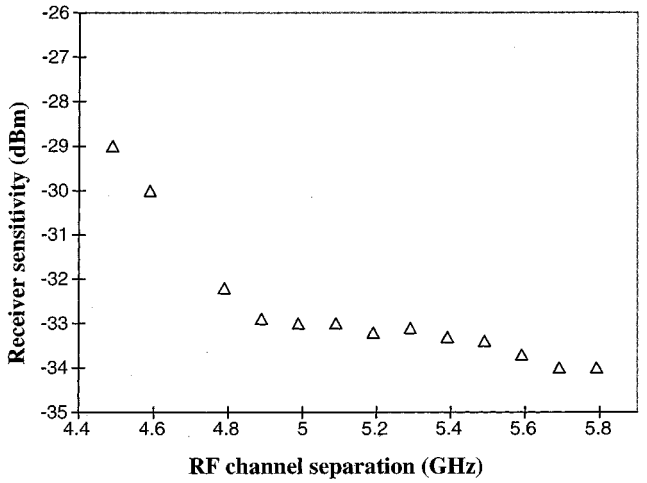

Fig. 6. Measured receiver sensitivity (at BER $= 10^{-9}$) versus frequency spacing between RF channels. Only two RF channels are used.

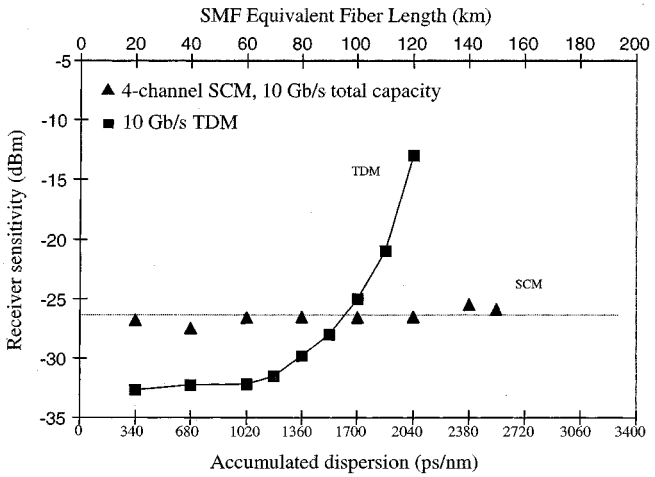

Fig. 7. Receiver sensitivity (at BER of 10^{-9}) comparison between a 10-Gb/s TDM system and a 4-tone SCM system with 10-Gb/s capacity.

persion of higher than 1700 ps/nm (corresponding to 100 km of SMF), the performance of the TDM system deteriorates rapidly, whereas the performance of the SCM system remains essentially unchanged. Because the transmission fiber used in our experiment has high negative dispersion, the effect of fiber nonlinear crosstalk may be underestimated.

III. Carrier Suppression

An important issue in an SCM system is intermodulation distortion. This mainly comes from nonlinear modulation characteristic of optoelectronic modulators. For an OSSB modulation using a dual-electrode MZ modulator, if the modulator is single-frequency modulated by $\cos(\Omega t)$, the output optical field is [8]

$$\begin{aligned} E_0 =& \frac{E_i}{2}\left\{\cos\left[\omega_c t + \frac{\pi}{2} + \beta\pi\cos\Omega t\right]\right. \\ &\left. + \cos\left[\omega_c t + \beta\pi\cos\left(\Omega t + \frac{\pi}{2}\right)\right]\right\} \\ =& \frac{E_i}{2}\left\{\sqrt{2}J_0(\beta\pi)\sin\left(\omega_c t - \frac{\pi}{4}\right)\right. \\ &- 2J_1(\beta\pi)\cos[(\omega_c+\Omega)t] \\ &+ 2J_2(\beta\pi)\sin[(\omega_c - 2\Omega)t] \\ &\left. + 2J_3(\beta\pi)\sin[(\omega_c - 3\Omega)t] + \cdots\right\} \end{aligned} \quad (1)$$

where $E_i(t)$ is the input optical field, $\omega_c = 2\pi f_c$ is the lightwave carrier frequency, Ω is the RF frequency of the modulation, and $\beta\pi = \pi V_{\rm ac}/V_\pi$ is the normalized amplitude of the RF drive signal. V_π is the switching voltage of the MZ modulator and $V_{\rm ac}$ is the amplitude of the sinusoid drive signal. Because MZ modulators do not have a linear transfer function, significant high-order harmonics can be generated if the modulation strength $\beta\pi$ is too high; this introduces crosstalk between channels. In practice, $\beta\pi \ll 1$ must be maintained so that the signal term $J_1(\beta\pi)$ is much higher than the higher order terms. For example, $\beta\pi$ must be smaller than 0.4 to guarantee that the signal power is 20 dB higher than the power of the second harmonic. However, at $\beta\pi = 0.4$, the power at the continuous wave (CW) carrier, represented by the $J_0(\beta\pi)$ term in (1), is approximately 11 dB higher than the signal. Obviously, a small modulation index means inefficient modulation and poor receiver sensitivity because the strong carrier component does not carry information. In order to increase the modulation efficiency while maintaining reasonably good linearity, optical carrier suppression may be applied using an optical notch filter. Fig. 8 illustrates the motivation of optical carrier suppression. Note that the carrier cannot be completely suppressed because the energy in the carrier must be equal to or higher than that of the signal. Otherwise, signal clipping will occur [9], which may introduce significant waveform distortion. In our experiment, we used an FP tunable filter in the reflection mode to perform optical carrier suppression.

The implementation of optical circuit for carrier suppression is shown in Fig. 9, where an optical circulator is used to catch the reflected lightwave signal from the FP filter and an active control is used on FP to stabilize the notch frequency at the optical carrier. To verify the effect of carrier suppression on system performance, we have measured the receiver sensitivity (at BER $= 10^{-9}$) for an SCM system with a single RF carrier and 2.5-Gb/s data rate. The power suppression ratio for the carrier was approximately 7 dB when the carrier suppression was applied. Fig. 10 shows the measured receiver sensitivity with and without carrier suppression. It is evident that the sensitivity improvement introduced by optical carrier suppression is inversely proportional to the RF power used to drive the electrooptic modulator. Although a calibration was not made between the RF power and the modulation index in our experiment, they should be directly proportional. Fig. 10 indicates that for high modulation indexes, the system performance improvement induced by carrier suppression is less than that seen with low modulation indexes. The reason is that, at high modulation index, the modulator already works in the nonlinear regime and carrier component is not a dominant term in the composite optical signal.

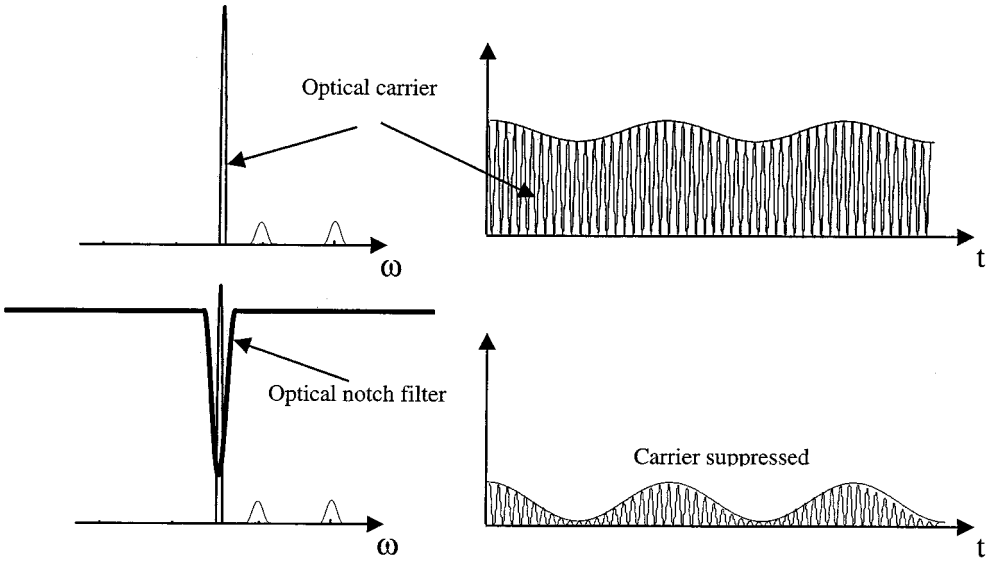

Fig. 8. Illustration of optical carrier suppression.

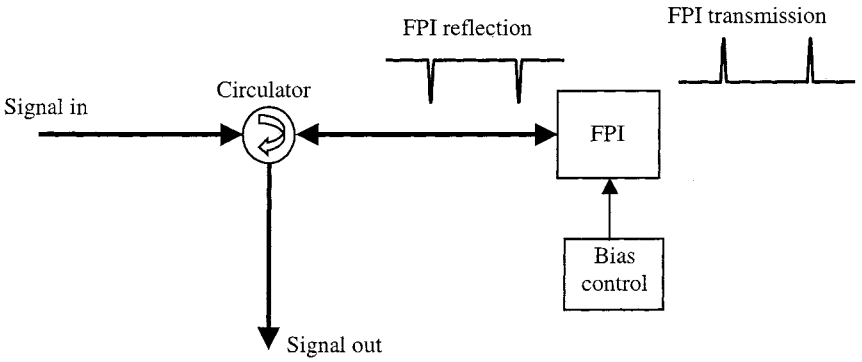

Fig. 9. Optical circuit for carrier suppression.

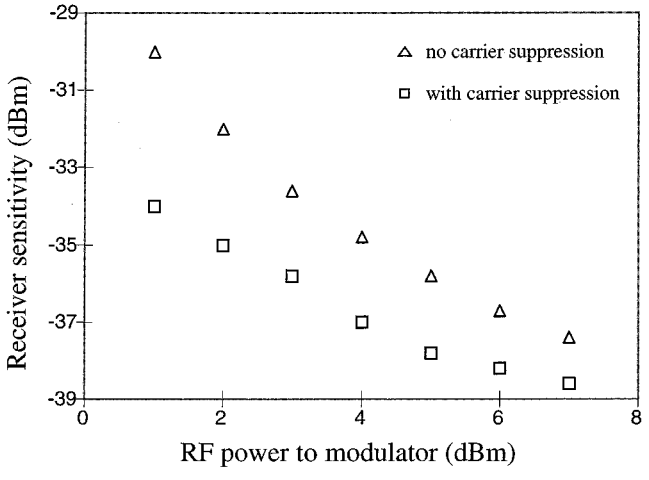

Fig. 10. Measured receiver sensitivity (at $\mathrm{BER} = 10^{-9}$) versus RF power used on the electrooptic modulator with and without optical carrier suppression. Only single RF channel is used at 8 GHz. Triangles: without carrier suppression. Squares: with approximately 7-dB optical carrier suppression.

IV. Receiver Sensitivity

In this section, we analyze the sensitivity of a digital SCM system with an optically preamplified receiver. A simplified block diagram of this system is shown in Fig. 11. In an SCM optical system with N subcarrier channels, similar to (1), the output electrical field from the electrooptic modulator is

$$E_0 = \frac{E_i}{2}\left\{\cos\left[\omega_c t - \sum_{k=1}^{N} u_k(t)\beta_k\pi \sin\Omega_k t\right] - \sin\left[\omega_c t + \sum_{k=1}^{N} u_k(t)\beta_k\pi\cos\Omega_k t\right]\right\} \quad (2)$$

where $u_k(t)$ is the normalized digital signal at the kth subcarrier channel. For PSK modulation, $u_k(t) = \pm 1$, and for ASK modulation, $u_k(t) = 0, 1$ to represent digital signal "0" and "1," respectively. ω_c is the carrier frequency and Ω_k is the RF subcarrier frequency of the kth channel.

In order to keep higher order harmonics small and operate the modulator in the linear regime, the modulation has to be weak. Under the assumption of small-signal modulation, $\left|\sum_{k=1}^{N}\beta_k\pi\right| \ll 1$ and (2) can be linearized as

$$E_0 = \frac{E_i}{\sqrt{2}}\left\{\sin\left(\omega_c t - \frac{\pi}{4}\right) - \frac{1}{\sqrt{2}}\sum_{k=1}^{N} u_k(t)\beta_k\pi\cos(\omega_c + \Omega_k)t\right\}. \quad (3)$$

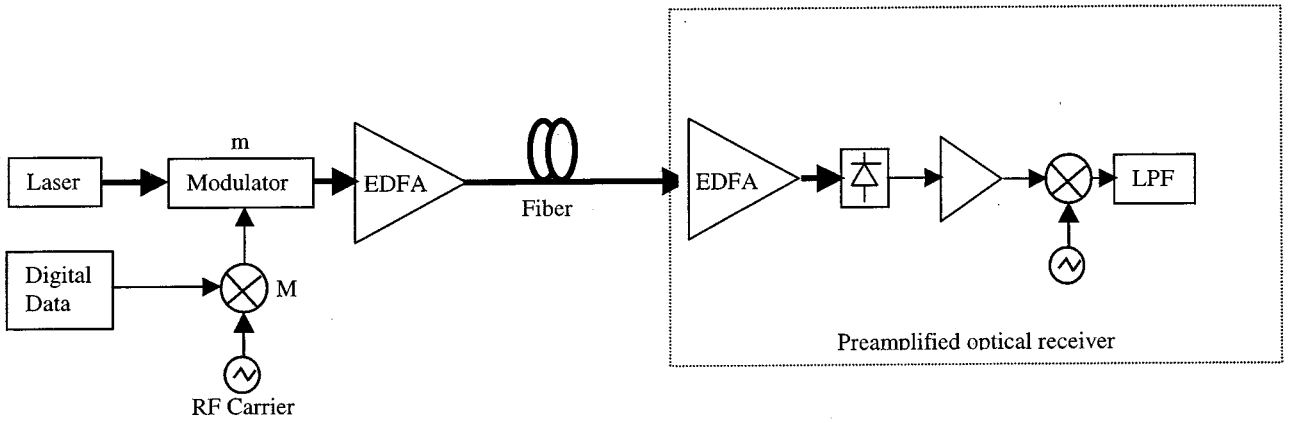

Fig. 11. Simplified block diagram of SCM system with amplified optical receiver.

Here, the first term in the bracket represents the carrier and the second term is the signal. If optical carrier suppression is considered, (3) can be modified as

$$E_0 = \frac{E_i}{\sqrt{2}}\left\{\sin\left(\omega_c t - \frac{\pi}{4}\right)\sqrt{\zeta} - \frac{1}{\sqrt{2}}\sum_{k=1}^{N} u_k(t)\beta_k \pi \cos(\omega_c + \Omega_k)t\right\} \quad (4)$$

where $0 \le \zeta \le 1$ is the power suppression ratio of the carrier. At the receiver, the optical carrier beats with the subcarriers at the photodiode, down-converting the optical subcarrier into the RF domain. The generated photocurrent at the receiver is

$$I_s = \eta |E_0|^2 G\Re \approx I_0\left\{1 + \frac{1}{\sqrt{\zeta}}\sum_{k=1}^{N} m_k u_k(t)\cos(\Omega_k t)\right\} \quad (5)$$

where η is the system transmission and coupling loss, $\Re$ is the photodiode responsivity, G is the gain of the optical preamplifier, $I_0 = \eta\zeta G\Re E_i^2/2 = P_{\text{in}}G\Re$ is the average photocurrent, P_{in} is the average power of the optical signal reaching the preamplified optical receiver, and $m_k = \sqrt{2}\beta_k\pi$ is the normalized modulation index. Obviously, the useful photocurrent signal for the kth channel is $I_k = P_{\text{in}}G\Re m_k u_k(t)\cos(\Omega_k t)/\sqrt{\zeta}$. In deriving (5), a small-signal approximation has been used. Receiver photocurrent must be positive; therefore

$$\left|\sum_{k=1}^{n} m_k u_k(t)\cos(\Omega_k t)\right| \le \sqrt{\zeta}. \quad (6)$$

Equation (6) sets a conservative approximation for the maximum amount of carrier suppression that can be applied without introducing clipping. In conventional analog SCM CATV systems with a large number of channels, clipping-induced signal-to-noise ratio (SNR) degradation is proportional to the power addition of all the channels [9]. In digital systems, however, the performance is measured by BER. Because of the nonlinear relationship between SNR and BER determined by an error function, a small degradation in SNR may induce a large BER change at low BER levels. Although (6) is a worst-case approach, it is appropriate for high-capacity digital systems with a limited number of channels.

In order to calculate the receiver sensitivity, amplified spontaneous emission (ASE) noise generated by the erbium-doped fiber amplifier (EDFA) preamplifier must be considered. The ASE noise spectral density is

$$\rho_{\text{ASE}} = 2n_{\text{sp}}h\nu(G-1) = Fh\nu(G-1) \quad (7)$$

where n_{sp} is the spontaneous emission factor, F is the noise figure of the EDFA, h is the Planck's constant, ν is the optical frequency, and G is the optical gain of the EDFA. Note that the factor 2 in front of n_{sp} is there to account for both polarizations of the ASE. After photodetection, the optical ASE noise is converted into the electronic domain. Consider only signal–ASE beat noise, which is usually the dominant noise source in an optically preamplified receiver. Under Gaussian approximation, the double-sideband electrical power spectral density of signal–ASE beat noise is

$$\langle i^2_{\text{sig-sp}}\rangle = \frac{1}{2}\Re^2 2\rho_{\text{ASE}}P_{\text{in}}G. \quad (8)$$

The factor 1/2 in (8) accounts for the fact that the signal has only a single polarization, and the factor 2 in (8) takes into account the double optical sidebands of the ASE noise (symmetric optical noise around the optical carrier). Because the noise is random, it can be decomposed into in-phase and quadrature components $n_c(t)$ and $n_s(t)$, respectively, and, thus, the total alternating current (ac) signal of the k-th RF channel entering the RF demodulator is

$$U_1 = \frac{P_{\text{in}}G\Re m_k u_k(t)\cos(\Omega_k t)}{\sqrt{\zeta}} + n_c(t)\cos(\Omega_k t) + n_s(t)\sin(\Omega_k t) \quad (9)$$

where the total noise power is

$$\frac{1}{2}\bar{n}_c^2 + \frac{1}{2}\bar{n}_s^2 = 2B_e\langle i^2_{\text{sig-sp}}\rangle = 2\Re^2\rho_{\text{ASE}}P_{\text{in}}GB_e, \text{ and } \bar{n}_c^2 = \bar{n}_s^2$$

where B_e is the spectral width of the signal baseband ($2B_e$ accounts for double RF sidebands).

At the RF demodulator, $U_1(t)$ coherently mixes with a local oscillator $2\cos(\Omega_k t)$, and the output of the demodulator is

$$U_2 = \frac{P_{\text{in}}G\Re m_k u_k(t)}{\sqrt{\zeta}} + n_c(t) \quad (10)$$

where frequency-doubled components have been filtered out. Assuming a reasonable optical gain of the EDFA preamplifier, $G \gg 1$, the SNR is

$$\text{SNR} = \frac{\frac{P_{\text{in}} G \Re m_k u_k(t)}{\sqrt{\zeta}}}{\sqrt{2\Re^2 P_{\text{in}} \rho_{\text{ase}} G B_e}} = \frac{\frac{P_{\text{in}} G \Re m_k u_k(t)}{\sqrt{\zeta}}}{\sqrt{2\Re^2 P_{\text{in}} F h\nu (G-1) G B_e}} \approx \sqrt{\frac{P_{\text{in}} m_k^2 u_k^2(t)}{2FhB_e\zeta}}. \tag{11}$$

It is worth mentioning that, in conventional intensity-modulation direct-detection optical systems, signal-dependent noise, such as signal-ASE beat noise, does not exist during signal "0." However, in SCM optical systems, receiver noise is identical at signal "1"s and "0"s as long as the frequency of the subcarrier is higher than the data rate it carries.

Using PSK modulation, and taking into account the fact that $u_k(t) \in (-1, 1)$, in the ideal case without signal waveform distortion, the receiver Q value can be approximated as

$$Q = \frac{\sqrt{P_{\text{in}}} m_k - (-1)\sqrt{P_{\text{in}}} m_k}{2\sqrt{2FhB_e\zeta}} = \frac{x\sqrt{P_{\text{in}}} m_k}{2\sqrt{2FhB_e\zeta}} \tag{12}$$

where $x = 2$ for PSK modulation.

For ASK modulation, $u_k(t) \in (0, 1)$ and for quadrature PSK (QPSK), $u_k(t) \in ((-1/\sqrt{2}), (1/\sqrt{2}))$; therefore, $x = 1$ for ASK and $x = \sqrt{2}$ for QPSK. To achieve a BER of 10^{-9} ($Q = 6$), the minimum required optical signal power must be

$$P_{\text{in}} = 288 \frac{hF\zeta B_e}{x^2 m_k^2}. \tag{13}$$

This value is commonly referred to as receiver sensitivity. In an SCM system, as the number of RF channels increases, the modulation index of each channel must decrease to satisfy (6). Assuming an identical modulation index for all RF channels, we have $\left(m_k/\sqrt{\zeta}\right) \leq 1/N$. In addition, the receiver electrical bandwidth B_e is determined by the data rate per RF channel. In a binary NRZ system, we can use $B_e = 0.7B/N$ where B is the total bit rate per subcarrier channel. Fig. 12 shows a practical example of receiver sensitivity versus the number of RF channels. In this example, the total data rate per wavelength is 10 Gb/s and the optical amplifier noise figure is 5 dB. As shown in Fig. 12, receiver sensitivity degrades as the number of subcarrier channels at each wavelength increases. This is mainly because of the decrease of the modulation index. For a BPSK system with $N = 4$, the minimum achievable receiver sensitivity is approximately -31 dBm.

In the sensitivity analysis presented so far, we have assumed that the optical bandwidth of the receiver is wide enough such that the optical noise is symmetric around the carrier, although optical signals are only at one side of the carrier because of the SSB modulation. If a narrowband optical filter is used in front of the receiver, optical noise on the mirror side of the optical signals may be removed and, therefore, the optical noise becomes single sided. Fig. 13 illustrates the effect of the narrowband optical receiver filter. If the bandwidth and center wavelength of the optical filter are properly arranged, the signal–ASE beat noise presented by (8) will be halved and the receiver sensitivity will be improved by 3 dB.

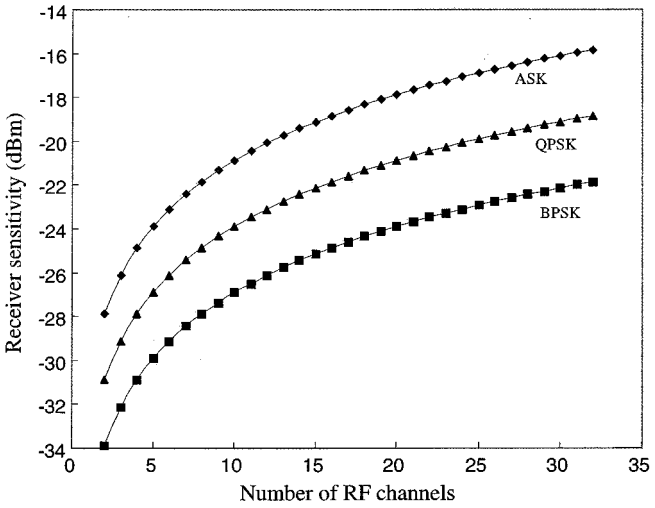

Fig. 12. Calculated receiver sensitivity versus the number of RF channels for ASK, BPSK, and QPSK modulation formats. Total data rate is 10 Gb/s and the optical amplifier noise figure is 5 dB.

It should be pointed out that the receiver sensitivity presented so far did not include signal waveform distortion and inter-channel crosstalk. Signal waveform distortion may be introduced by nonideal transfer function of RF circuitry and optical modulator, chromatic dispersion, self-phase modulation (SPM), and PMD. In an SCM optical system using OSSB modulation, because the datarate per subcarrier channel is low, the system tolerance to chromatic dispersion is increased by N^2 compared to a conventional TDM system at the same data rate per wavelength. SPM depends on the optical power per subcarrier, with a fixed optical power per wavelength; the effect of SPM will decrease with N. However, we will show, in Section VI, that PMD is likely a limiting factor in SCM optical systems. In addition, with a fixed optical modulator bandwidth, increasing the number of RF channels will decrease the frequency spacing between them. Although linear crosstalk can be minimized using high-quality microwave filters, nonlinear crosstalk created during the transmission in the optical fiber may become significant. This will be discussed in the Section V.

V. Crosstalk Created by Fiber Nonlinearity

XPM and FWM are two of the most important sources of nonlinear crosstalk in multiwavelength fiber-optic systems. Their effects are generally proportional to signal optical power and inversely proportional to the channel spacing [10], [11]. In contrast to a conventional WDM system, an SCM optical system packs low data-rate RF channels tightly within the available modulation bandwidth of an optical modulator, and the optical power per RF channel is relatively low. The understanding of nonlinear crosstalk optical SCM systems is critical in the system design.

In the following evaluation, we assume that the total data rate carried by one wavelength is 10 Gb/s, the total RF bandwidth of the modulator is 20 GHz, the total optical power is 4 mW after

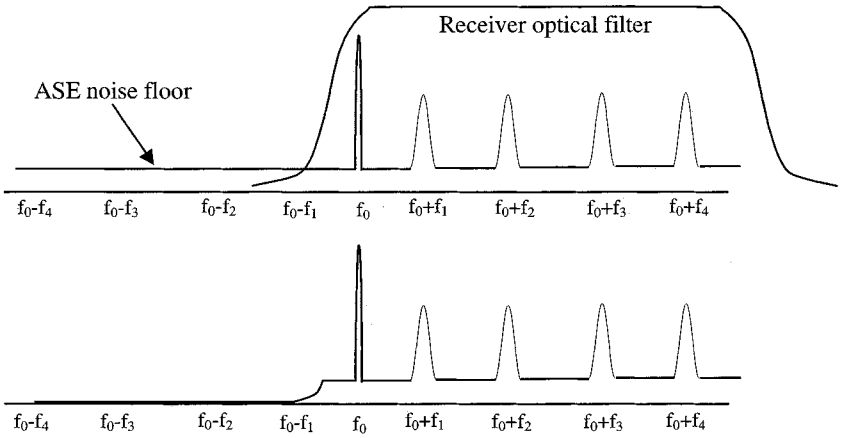

Fig. 13. Illustration of receiver noise reduction by using a tuned narrowband optical filter.

each optical amplifier, and each RF subcarrier has the same optical power and data rate. We use a Gaussian approximation to quantify the level of nonlinear crosstalks due to XPM and FWM and evaluate their standard deviations normalized to the optical signal. For simplicity, we assume a nondispersion-compensated optical system with five optically amplified fiber spans; each has 80 km of optical fiber and only the performance at the center channel is evaluated because it usually has the strongest nonlinear crosstalk.

The evaluation of XPM crosstalk follows the analysis in [11]. Fiber dispersion and, thus, the relative walk-off between adjacent RF channels, represented by $d_{jk} = D\Delta\lambda_{jk}$, is an important parameter to determine XPM crosstalk. $d_{jk} \gg \beta_2\Omega/2$ was assumed in [11], but is no longer valid here because the modulation data rate is comparable to the frequency spacing between RF channels. In the aforementioned expressions, D is the fiber dispersion parameter, λ and $\Delta\lambda_{jk}$ are the average wavelength and the wavelength separation between adjacent RF channels, respectively, $\beta_2 = -(\lambda^2/2\pi c)D$ is the dispersion coefficient, Ω is the baseband frequency, and c is the speed of light. In a system with N RF channels and M optical amplified fiber spans, the normalized noise power generated at the jth channel by XPM is

$$\sigma^2_{\text{xpm}} = \sum_{k=1,k\neq j}^{N} \left\{ \int_0^{\infty} \Delta p_{jk}(\Omega, L_M)\sqrt{H(\Omega)}d\Omega \right\} \quad (14)$$

with

$$\begin{aligned}\Delta p_{jk}(\Omega, L_M) &= \left| \sum_{i=1}^{M} \left\{ 2\gamma_i p_k^{(i)}(\Omega, 0) \exp\left[i\Omega \sum_{n=1}^{i-1} d_{jk}^{(n)} L^{(n)} \right] \right.\right. \\ &\quad \times \left\{ \frac{\exp\left(\frac{i\beta_2\Omega^2 L_i}{2}\right) - \exp(-\alpha + i\Omega d_{jk})L_i}{i\left(\alpha - i\Omega d_{jk} + \frac{i\beta_2\Omega^2}{2}\right)} \right. \\ &\quad \left.\left. \left. - \exp \frac{\left(\frac{-i\beta_2\Omega^2 L_i}{2}\right) - \exp(-\alpha + i\Omega d_{jk})L_i}{i\left(\alpha - i\Omega d_{jk} - \frac{i\beta_2\Omega^2}{2}\right)} \right\} \right\} \right|^2. \end{aligned} \quad (15)$$

Here, $H(\Omega)$ is the receiver electrical power transfer function, α is the attenuation coefficient of the fiber, L_i is the length of the ith fiber span, and L_M is the accumulated fiber length of the whole system. $\gamma_i = 2\pi n_2/(\lambda_j A_{\text{eff}})$ is the nonlinear coefficient, n_2 is the nonlinear refractive index, λ_j and λ_k are the RF channel wavelengths, A_{eff} is the fiber effective core area, and $p_k = |A_k|^2$ and $p_j = |A_j|^2$ are optical powers of the pump and the probe RF channels, respectively.

In an SCM optical system, we assume 50% of the optical power is in the carrier. Because the carrier is always CW, it does not contribute to XPM. Fig. 14(a) shows the normalized standard deviation due to XPM. The plot starts from two RF channels (with 5-Gb/s data rate per RF channel and 10-GHz channel spacing) and ends with 32 RF channels (with 312.5-MHz data rate per RF channel and 625-MHz channel spacing). Fig. 14(a) demonstrates that, with the increase in the number of channels, the XPM crosstalk decreases monotonically. The effect of decreased channel spacing is approximately compensated by the decrease of signal optical power per channel. On the other hand, because the XPM spectral transfer functions have typically high-pass characteristics, especially at low frequencies [11], the decrease of channel data rate and, thus, the decrease of the baseband filter bandwidth, reduced the effect of XPM crosstalk at the large RF channel counts. Due to interference between XPM created by various amplified fiber spans, the XPM contribution versus channel spacing is usually not monotonic at small number of channels; this can also be explained by the nonuniformity of XPM spectral transfer function in the frequency domain [11].

FWM is another source of nonlinear crosstalk created by Kerr effect in optical fibers. Assume that all beating components around the signal frequency f_j are within the receiver bandwidth. Three channels, j, k, and l, beat to generate a crosstalk at the nth channel. The frequency relation has to satisfy $f_{jkl} = f_n = f_j + f_k - f_l, l \neq j, k$. Using small-signal approximation, assuming equal channel power and equal channel spacing, the crosstalk power generated by FWM has a simple expression

$$\sigma^2_{\text{fwm}} = \sum_{jkl} \frac{4P^2\gamma^2 G^2_{jkl}}{\alpha^2 + \Delta\beta^2_{jkl}} x_{jkl} \quad (16)$$

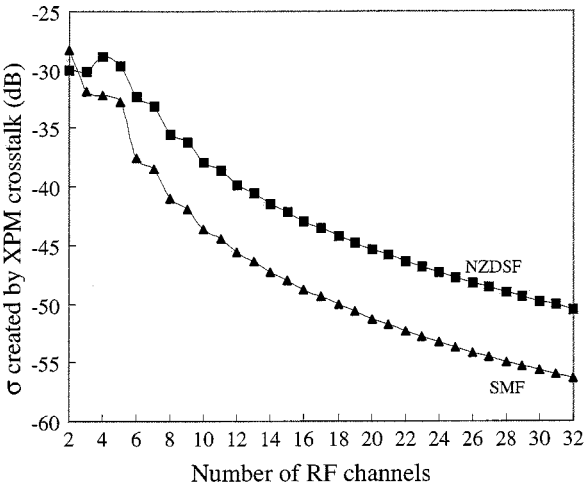

(a)

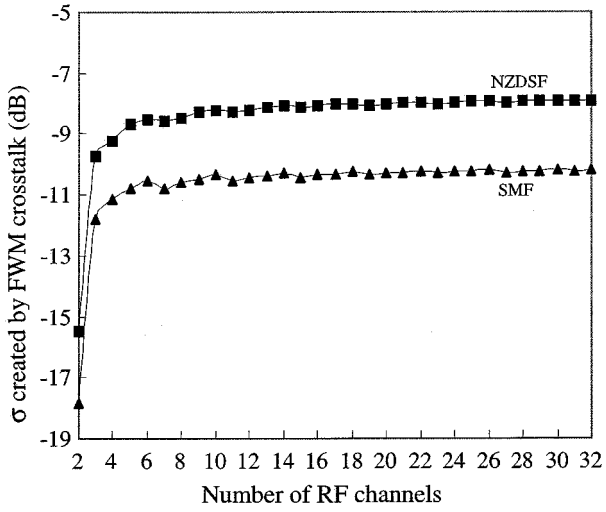

(b)

Fig. 14. Calculated (a) XPM and (b) FWM crosstalk in SCM systems. Total data rate is 10 Gb/s and total RF bandwidth is 20 GHz. Five amplified spans each have 80 km of fiber, and the EDFA output optical power is 4 mW.

with

$$\Delta\beta_{jkl} = \frac{2\pi\lambda^2 D}{c}(f_j - f_l)(f_k - f_l) \tag{17}$$

where $G_{jkl} = 1$ for two-tone products and $G_{jkl} = 2$ for three-tone products. P is the optical power per RF channel and x_{jkl} represents a combined effect of the relative phase between the contributing waves and the statistics of the data signal [12]. In SCM optical systems with RF phase modulation, such as PSK, signal has the same optical power for digital "0"s and "1"s. The random phase relationship between different contributing waves is $x_{jkl} = 1/2$ if all the powers are the same. However, in an SCM optical system, the CW optical carrier contains at least half of the total optical power, $P_{\text{carrier}} = MP$, where M is the number of RF channels per wavelength, P is the optical power per RF channel, and P_{carrier} is the optical power of the carrier. Although the CW carrier does not contribute to the XPM process, it must be considered in FWM analysis because of its high optical power. We can simply set $x_{jkl} = M/2$ if any one of j, k, and l represents the carrier.

Fig. 14(b) shows the normalized standard deviation due to FWM. Because the effect of FWM is proportional to the signal optical power and inversely proportional to the square of the channel spacing, it generally increases with the increase of the number of channels, as shown in Fig. 14(b). However, when the RF channel spacing is too small, there is negligible walk-off within the fiber nonlinear length. If $\alpha > \Delta\beta_{jkl}$, σ_{fwm} will no longer increase with the number of channels.

Comparing Fig. 14(a) and (b), it is evident that FWM is the major source of nonlinear crosstalk in SCM optical systems with low data rate per channel and extremely narrow spacing between RF channels. Although a low optical power level is desired for the reduction of FWM crosstalk, it hurts the system by reducing the SNR at the receiver. The estimation of maximum transmission distance of the system may require numerical simulations, which optimize optical power level according to the characteristics of optical amplifiers, optical fibers, dispersion compensation strategies, the number of wavelengths, and the number of RF channels per wavelength. PMD characteristic of the transmission fiber is also a big concern.

VI. Effect of PMD

It has been recognized, in recent years, that in high-speed fiber-optic transmission systems, PMD is one of the important sources of performance degradation. The phenomena of PMD can be easily explained in the time domain. An optical signal in a fiber is decomposed into two orthogonal polarization modes, and each of them travels in slightly different speeds. This causes a differential group delay (DGD) of the optical signals and, thus, introduces signal waveform distortion at the receiver. The generally accepted limit for DGD is about 15% of the bit time for the nonreturn-to-zero (NRZ) modulation format [13].

Another, yet equivalent, explanation of PMD is in the frequency domain, where we consider that two lightwave signals with slightly different wavelengths are launched into an optical fiber. Although the two lightwave signals have the same state of polarization (SOP) at the fiber input, their SOPs may walk off from each other after propagating through the fiber. This SOP walk-off is caused by PMD, and is proportional to both wavelength separation between the two lightwave signals and the DGD of the fiber.

In an SCM optical system, the composite electrical signal at the receiver is produced by the heterodyne beating between the carrier and the subcarriers. In order to maintain a stable and acceptable level of electrical signal at the receiver, the SOPs must be aligned between the carrier and the subcarrier. Any SOP walk-off will introduce fading in the beating signal. If the frequency separation between the carrier and the subcarrier is $\Delta\omega$ in radians and the DGD of the fiber system is $\Delta\tau$ in seconds, then the angle separation of SOP between these two frequency components on the Poincaré coordinate is

$$\Delta\theta = \Delta\tau \cdot \Delta\omega.$$

This formula has been used in fiber PMD measurements, and it is commonly referred to as the fixed-analyzer method [14].

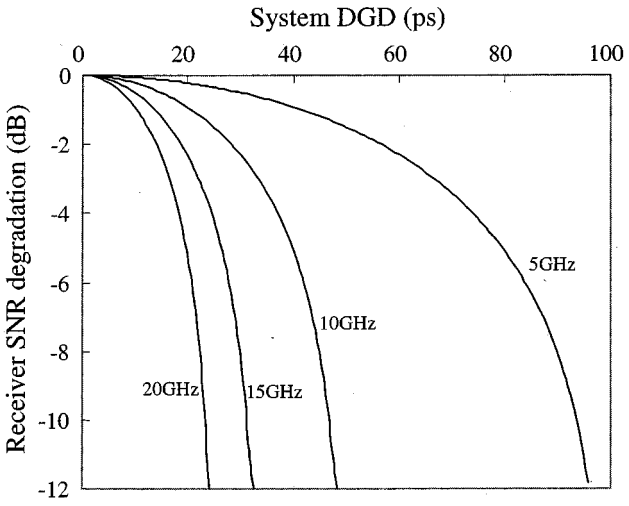

Fig. 15. Calculated receiver sensitivity penalty caused by PMD for subcarrier channels with several different RF frequencies.

Because of this SOP walk-off, the electrical signal at the receiver is decreased by a factor

$$A = \cos\left(\frac{\Delta\theta}{2}\right) = \cos\left(\Delta\tau \cdot \frac{\Delta\omega}{2}\right). \tag{18}$$

Because the noise at the receiver is not affected by this SOP walk-off, A is also the degradation factor of the receiver SNR. Fig. 15 shows the SNR degradation versus the accumulated system DGD. As an example, for 1-dB SNR degradation $(A = -1 \text{ dB})$ and 15-GHz carrier–subcarrier separation, the required system DGD must be smaller than 10 ps. It is worth mentioning that the SOP walk-off induced SNR degradation is, to the first order, independent of the data rate on each RF subcarrier; it only depends on the frequency separation between the carrier and the subcarrier. This is indeed a stringent limitation for the system.

This signal fading can also be explained in the time domain [15]. During fiber transmission, both the carrier and the subcarrier are decomposed into fast and slow principal states of polarization (PSPs). This causes a phase difference in the received subcarrier signal at the photodiode. If we assume an equal amount of optical power is distributed into the fast and slow PSPs, the received subcarrier component in the RF domain is

$$\begin{aligned} I(t) =& 0.5a(t)[\cos(\Delta\omega t) + \cos(\Delta\omega t + \Delta\omega\Delta\tau)] \\ =& a(t)\cos\left[\Delta\omega\left(t + \frac{\Delta\tau}{2}\right)\right] \cdot \cos\left(\Delta\omega \cdot \frac{\Delta\tau}{2}\right) \end{aligned}$$

where $a(t)$ is the data signal carried by the subcarrier. Obviously, the PMD-induced subcarrier fading is proportional to $\cos(\Delta\omega \cdot \Delta\tau/2)$, which is identical to the amount of fading described by the polarization walk-off. Although the subcarrier fading can be explained in two seemingly quite different ways, they originate from the same physical mechanism and the effect should not be counted twice.

VII. Conclusion

We have analyzed the performance of fiber-optic SCM transmission using OSSB both experimentally and theoretically. OSSB is an effective method to reduce the impact of fiber chromatic dispersion and increase bandwidth efficiency. Receiver sensitivity has been evaluated for SCM systems using an optically preamplified receiver, and a comparison has been made between different modulation formats. Optical carrier suppression was suggested to increase modulation efficiency while keeping MZ modulator intermodulation crosstalk low. Because, in SCM systems, frequency spacing between adjacent RF channels is much narrower than that in a conventional DWDM system, we have evaluated the effect of nonlinear crosstalk in optical fibers created by XPM and FWM. We have demonstrated that FWM is the dominant source of nonlinear crosstalk in SCM optical systems. Although chromatic dispersion is not a limiting factor in SCM systems, PMD has a big impact in the system performance if RF coherent detection is used in the receiver. In order to optimize the system performance, tradeoffs must be made between data rate per subcarrier, levels of modulation, channel spacing between subcarriers, optical power, and modulation indexes. A 10-Gb/s SCM test bed has been set up in which 4×2.5 Gb/s data streams are combined into one wavelength, which occupies a 20-GHz optical bandwidth. OSSB modulation is used in the experiment. The measured results agree well with the analytical prediction.

References

[1] M. R. Phillips and T. E. Darcie, "Lightwave video transmission," in *Optical Fiber Telecommunications*, I. P. Kaminon and T. L. Koch, Eds. New York: Academic, 1997, vol. IIIA.

[2] P. M. Hill and R. Olshansky, "A 20-channel optical communication using subcarrier multiplexing for the transmission of digital video signals," *J. Lightwave Technol.*, vol. 8, pp. 554–560, Apr. 1990.

[3] K. P. Ho, H. Dai, C. Lin, S.-K. Liaw, H. Gysel, and M. Ramachandran, "Hybrid wavelength-division-multiplexing systems for high-capacity digital and analog trunking applications," *IEEE Photon. Technol. Lett.*, vol. 10, pp. 297–299, Feb. 1998.

[4] P. A. Greenhalgh, R. D. Abel, and P. A. Davies, "Optical prefiltering in subcarrier systems," *Electron. Lett.*, vol. 28, p. 2054, Nov. 1992.

[5] R. Hui, B. Zhu, R. Huang, C. Allen, K. Demarest, and D. Richards, "10 Gb/s SCM system using optical single side-band modulation," in *Proc. OFC'01*, Anaheim, CA, Mar. 2001, MM4.

[6] M. E. Frerking, *Digital Signal Processing in Communication Systems*. New York: Chapman & Hall, 1994.

[7] J. Conradi, B. Davis, M. Sieben, D. Dodds, and S. Walklin, "Optical signal sideband () transmission for dispersion avoidance and electrical dispersion compensation in microwave sub-carrier and baseband digital systems," *Electron. Lett.*, vol. 33, pp. 971–973, May 1997.

[8] G. H. Smith, D. Novak, and Z. Ahmed, "Overcoming chromatic dispersion effects in fiber-wireless systems incorporating external modulators," *IEEE Trans. Microwave Technol.*, vol. 45, pp. 1410–1415, Aug. 1997.

[9] N. J. Frigo, "Clipping distortion in lightwave CATV systems: Models, simulations and measurements," *J. Lightwave Technol.*, vol. 11, pp. 138–146, Jan. 1993.

[10] K. Inoue, K. Nakanishi, K. Oda, and H. Toba, "Crosstalk and power penalty due to fiber four-wave mixing in multichannel transmissions," *J. Lightwave Technol.*, vol. 12, pp. 1423–1439, Aug. 1994.

[11] R. Hui, K. Demarest, and C. Allen, "Cross phase modulation in multi-span WDM optical fiber systems," *J. Lightwave Technol.*, vol. 17, pp. 1423–1439, Aug. 1994.

[12] M. Eiselt, "Limits on WDM systems due to four-wave mixing: A statistical approach," *J. Lightwave Technol.*, vol. 17, pp. 2261–2267, Nov. 1999.

[13] S. Lanne, D. Penninckx, J.-P. Thiery, and J.-P. Hamaides, "Extension of polarization-mode dispersion limit using optical mitigation and phase-shaped binary transmission," in *Proc. OFC'00*, Baltimore, MD, Mar. 7–10, 2000, ThH3.

[14] D. Derickson, Ed., *Fiber Optic Test and Measurement*. Upper Saddle River, NJ: Prentice-Hall, 1998.

[15] O. H. Adamczyk, A. B. Sahin, Q. Yu, S. Lee, and A. E. Willner, "Statistics of PMD-induced power fading for double sideband and single sideband subcarrier-multiplexed signals," in *Proc. OFC'01*, Anaheim, CA, Mar. 19–22, 2001, MO5.

Rongqing Hui (A'94–M'97–SM'97) received the B.S. degree in microwave communications and the M.S. degree in Lightwave Technology from Beijing University of Posts and Telecommunications, Beijing, China, in 1982 and 1988, respectively, and the Ph.D. degree in electrical engineering from the Politecnico di Torino, Torino, Italy, in 1993.

From 1982 to 1985, he taught at the Physics Department of Anhui University, Hefei, China, where he also conducted research on optical fibers and fiber sensors. From 1985 to 1989, he was with the Optical Communication Laboratory of the Beijing University of Posts and Telecommunications, where he worked in coherent optical fiber communication systems and components. From 1989 to 1990, he held a research fellowship from the Fundazione Ugo Bordoni, Rome, Italy, working on nonlinear effects and optical injection locking of semiconductor laser devices. From 1990 to 1993, he was with the Department of Electronics, Politecnico di Torino, where he worked on optical communications and single frequency semiconductor laser devices. During this period, he also held a fellowship from Telecommunication Research Center (CSELT), Torino, Italy, where his research subject was polarization-insensitive coherent optical communication systems. He spent one year, from 1993 to 1994, as a Postdoctoral Research Fellow working on optical systems and networks architecture at the University of Ottawa, Ottawa, ON, Canada. In 1994, he became a Member of Scientific Staff at Bell-Northern Research (now part of Nortel), Ottawa, where he has worked in the research and development of high-speed optical transport networks. Since September 1997, he has been a faculty member in the Electrical Engineering and Computer Science Department, University of Kansas, Lawrence. As an author or coauthor, he has published more than 70 technical papers in the area of fiber-optic communications. He also holds a number of patents. He currently serves as an Associate Editor of IEEE TRANSACTIONS ON COMMUNICATIONS.

Benyuan Zhu, photograph and biography not available at the time of publication.

Renxiang Huang received the B.S. degree in electrical engineering from Beijing University of Posts and Telecommunications (BUPT), Beijing, China, in 1993 and the M.S. degree in electrical engineering from University of Kansas, Lawrence, in 2001.

From 1993 to 1998, he worked as a Research and Development Engineer in the Optical Communications Laboratory of BUPT. He was engaged in the development of coherent, WDM, OTDM, and CATV systems. In 1998, he joined the Lightwave Laboratory of the University of Kansas as a Research Assistant working on the research of optical SCM systems. From August to April 2001, he worked at Cisco Systems as a Software Engineer. In June 2001, he became a Research Engineer at the Lightwave Laboratory and was engaged in the research of PMD mitigation and simulation of DWDM transmission in the lightwave lab. Since November 2001, he has been a Research and Development Engineer with Sprint Advanced Technology Laboratories, Burlingame, CA.

Christopher T. Allen (M'94–SM'95) was born in Independence, MO, on October 7, 1958. He received the B.S., M.S., and Ph.D. degrees in electrical engineering from the University of Kansas, Lawrence, in 1980, 1982, and 1984, respectively.

From 1984 to 1990, he was with Sandia National Laboratories, Albuquerque, NM, working in exploratory radar systems and development of high-speed digital systems. From 1990 to 1994, he was with the Allied Signal Kansas City Division, Kansas City, MO, where he worked in the areas of high-speed digital design, radar systems analysis, and multichip module development. Since August 1994, he has been a faculty member in the Electrical Engineering and Computer Science Department at the University of Kansas. His research interests include high-speed digital circuits, microwave remote sensing, radar systems, and photonics and lightwave technologies. He has served as a technical reviewer for several IEEE journals, as well as *Remote Sensing of the Environment*, *Geophysics—The Journal of the Society of Exploration Geophysicists* and *Journal of Glaciology*. He currently is the Director of the Radar Systems and Remote Sensing Laboratory and Co-Director of the Lightwave Communication Systems Laboratory, University of Kansas. He also serves on the Society of Automotive Engineers International AE-8D task group on standards development for Fiber Optic Cable and Test Methods for aerospace applications.

Dr. Allen is a member of Phi Kappa Phi, Tau Beta Pi, Eta Kappa Nu, and the International Union of Radio Science (URSI).

Kenneth R. Demarest (S'78–M'79–SM'99) was born in Hackensack, NJ, on December 16, 1952. He received the B.S. degree in electrical engineering from John Brown University, Siloam Springs, AR, in 1974 and the M.S. and Ph.D. degrees in electrical engineering from Ohio State University, Columbus, in 1976 and 1980, respectively.

From 1974 to 1979, he was a Graduate Research Associate with the ElectroScience Laboratory at Ohio State University. From 1979 to 1984, he was an Assistant Professor in the Electrical Engineering Department of Lafayette College, Easton, PA. Since 1984, he has been with the Electrical Engineering and Computer Science Department at the University of Kansas, Lawrence, most recently as a Professor. His research interests are in the areas of fiber-optic communications and electromagnetics. He is the author of a number of papers, book chapters, and the book *Engineering Electrotnagnetics*.

Dr. Demarest is a member Eta Kappa Nu and the International Union of Radio Science (URSI) Commission B.

Douglas Richards received the B.S. and M.S. degrees in electrical engineering from the University of Missouri, Rolla.

In 1998, he joined Sprint, Inc., Overland Park, KS, initially working in the Optical Engineering & Standards department. He is currently a Senior Member of the Technical Staff within Technology Planning and Integration (TP&I), Sprint, Overland Park, KS. He works at the physical transport layer, exploring fiber compatibility issues and technologies that would improve long-haul transmission efficiencies. Part of his responsibility is to comanage TP&I's research in this area, i.e., lightwave projects at University of Kansas, Lawrence. More recently, he supports Sprint's efforts to explore last mile access solutions to include local multipoint distribution systems and optical wireless technologies. He is a principal contributor to Sprint's Optical Networking request for proposal, calling for a network overlay for core transmission to more efficiently support growing bandwidth-length demands and quality-of-service guarantees. He represents Sprint in the ITU-T SG-15/Q.16&17.